JOURNAL OF APPLIED ELECTROCHEMISTRY 19 (1989) 127–135

The discharge behaviour of the porous lead electrode in the lead–acid battery. I. Experimental investigations

P. EKDUNGE[1]*, D. SIMONSSON[2]

[1]*Department of Chemical Technology and* [2]*Department of Applied Electrochemistry and Corrosion Science, The Royal Institute of Technology, S-100 44 Stockholm, Sweden*

Received 4 December 1987; revised 31 August 1988

The discharge kinetics of the porous lead electrode have been investigated experimentally as a function of extent of discharge and the concentration of lignosulphonate expander. The results show that the kinetic model previously suggested for the recharge reaction can also be fitted to the anodic polarization curves. The structural changes in the electrode have been studied with SEM and electron microprobe analysis. These studies show that the higher discharge capacity at higher discharge currents of electrodes with organic expander in comparison to electrodes without expander is due to the formation of larger lead sulphate crystals in the former case. The discharge capacity at high current density (1000 A m^{-2}) is limited by depletion of sulphuric acid in the pores only at concentrations lower than the normal.

1. Introduction

The porous lead electrode is of great importance as the negative electrode in the lead–acid battery. Its electrochemistry in sulphuric acid has been reviewed by Hampson and Lakeman [1], Mahato [2] and Pavlov [3]. At high rates and low temperatures the discharge process of the lead–acid battery is limited by the negative electrode [4]. The possible limiting factors are: (i) coverage of the electroactive surface by precipitated lead sulphate; (ii) depletion of sulphuric acid in the pores; (iii) insufficient utilization of interior active material due to pore-mouth blocking; (iv) loss of electronic conductivity of the active mass.

Hullmeine and Kappus [5] demonstrated the effects of acid depletion and acid concentration on active mass utilization in both the positive and negative electrode by forcing flow of electrolyte through the porous electrode as in Liebenow's classical experiment [1]. Winsel *et al.* [6] observed 'ice passivation' of the porous lead electrode at −18° C. Asai *et al.* [7] concluded that plugging of the pores is the predominating limitation at lower electrolyte concentrations, whereas at higher electrolyte concentrations the coverage by lead sulphate is the limiting factor.

The high rate, low temperature performance is improved by addition of expander [4, 8–13], which also increases the cycle life of the electrode [8, 13–15], makes the lead crystals smaller and increases the surface area [8–10]. According to some authors [10, 11] the lead sulphate crystals become smaller in the presence of the expander, while others have reported the opposite effect [17–19] and still others no substantial effect at all on the size of the lead sulphate crystals [3]. The expander has been suggested to suppress the solid state passivation [8, 12, 15, 20].

The electrochemical kinetics have been studied on both planar and porous electrodes [12, 20–33]. The electrochemical reaction proceeds via a dissolution–precipitation mechanism at lower overvoltages. At higher anodic overvoltage a solid state reaction occurs. For the anodic reaction Tafel slopes in the region of 25–40 mV $decade^{-1}$ have been reported [20, 22, 23, 27–29]. Kabanov [21] observed a lower value of 15 mV $decade^{-1}$ at low current densities. Addition of lignin-type expander increases the Tafel slope from about 30 to about 45 mV for a solid lead electrode in 1 M H_2SO_4 [20].

The structural changes in the porous lead electrode have been studied with a scanning electron microscope by Pavlov and Iliev [14, 34] and by Asai *et al.* [7]. The lead sulphate distribution across the porous electrode has been determined experimentally by means of X-ray microprobe analysis by Asai *et al.* [7] and by Panesar and Portscher [35].

Winsel *et al.* [6, 36] have worked out a mathematical model, which describes the passivation of the lead electrode by a diaphragm of lead sulphate crystals hindering the diffusion of lead ions from the lead surface.

In spite of the numerous investigations that the porous lead electrode has been subjected to, there is still a need for more knowledge as a basis for explanations and predictions of the electrode behaviour, with its complex interacting effects of electrochemical kinetics, structural changes and mass transfer processes. The purpose of this paper is to study experimentally the mass utilization in the porous lead electrode in sulphuric acid and to experimentally estimate the values of parameters which are needed in a mathematical model for the porous lead electrode.

* *Present address*: Dechema-Institute, Theodor-Heuss-Allee 25, 6000 Frankfurt, M.27, FRG.

0021-891X/89 $03.00 + .12

2. Experimental details

The investigations were performed with three different types of lead electrodes: electrodes without any organic expanders, electrodes with 0.08% sodium lignosulphonate and electrodes with 0.3% lignosulphonate. The electrodes with no and with 0.3% organic expander were prepared as described in [37]. The electrodes with the medium, standard concentration of organic expander were factory manufactured and supplied dry-charged from Tudor AB, Sweden. Details in the design of the electrodes and the experimental procedure have been reported elsewhere [38]. The experiments were performed at room temperature (22 ± 1° C). The discharge current was interrupted at −0.6 V vs the Hg/Hg_2SO_4 reference electrode. The amount of discharge was measured with an electronic computer. All experiments were carried out between the third and tenth discharge–charge cycles.

The lead sulphate distribution across the cross section of the electrode was measured with an electron probe microanalyser (ARL SEMQ 42) by recording the intensity of S–K_α radiation. The morphologies of the lead and lead sulphate structures were studied with a scanning electron microscope (JEOL, JSM 840). Before samples were taken for SEM and electron probe microanalyses the electrodes were washed in acetone in three steps and dried in a vacuum oven at 40° C.

3. Results

3.1. *Discharge capacity*

Galvanostatic discharge curves are plotted in Fig. 1 as overvoltage vs charge output, $q = it$, for the three different electrodes. The curves are corrected for the ohmic voltage drop in the solution between the electrode and the Luggin capillary. For the high rate discharges with 1000 A m^{-2}, the recovered capacity after a rest period of 30 min after the end of discharge was measured by repeated discharge with the same current density. This second discharge is also shown in Fig. 1. All the electrodes had about the same capacity when they were discharged with a low current density. On the other hand, when the electrodes were discharged with a high current density, the electrode without organic expander had only about half the discharge capacity of the electrodes with expander. The recovered capacity after a discharge with 1000 A m^{-2} and a rest period of 30 min also increased with increasing concentration of expander. At the second discharge with 1000 A m^{-2} the electrode potential initially jumped to approximately the same value as in the first discharge for each electrode, but then increased much faster. For the electrodes with expander a slight second arrest at an overvoltage of about 0.2 V was observed.

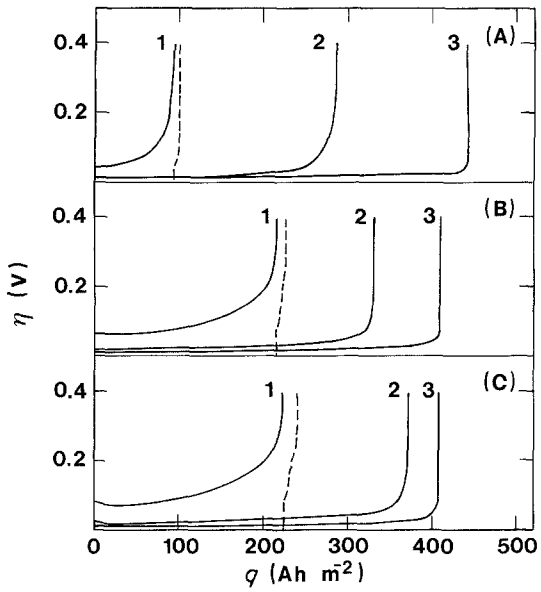

Fig. 1. Change in overvoltage during discharge at different current densities, 1000 A m^{-2} (1), 100 A m^{-2} (2) and 20 A m^{-2} (3). (A) Electrode without expander; (B) electrode with 0.08% expander; (C) electrode with 0.3% expander. Dashed lines: continued discharge after a rest period of 30 min.

The effect of the electrolyte concentration on the discharge capacity is shown in Table 1. For low electrolyte concentrations the capacity increases strongly with increasing electrolyte concentration, which indicates that electrolyte depletion is the capacity limiting process in this case. Close to the normal concentration of about 5 M H_2SO_4 the dependence is much smaller. During discharge the concentration of sulphuric acid in the pores decreases continously due to a limited diffusion rate. At high current densities this can lead to acid depletion, which limits the discharge capacity. The effect of the limited diffusion rate was measured by a determination of the concentration of sulphuric acid in the pores at the end of discharge. This was done by taking the electrode out of the cell immediately after the discharge was interrupted, absorbing the electrolyte on the external surface with paper tissue and leaching out the pore electrolyte with acetone in three steps. The amount of sulphuric acid in the leaching solution was determined by titration with NaOH. In this way the mean concentration of sulphuric acid in the pores of the standard electrode at the end of a discharge with 1000 A m^{-2} was determined to 3.0 M. If a linear concentration profile of sulphuric acid is assumed, which is a conservative estimate, the concentration of sulphuric acid in the centre of the electrode will be 1 M at the end of discharge and there will be enough sulphuric acid for further discharge.

3.2. *Kinetic model*

Anodic polarization curves for the three different elec-

Table 1. Discharge capacity at different concentrations of sulphuric acid. Current density = 1000 A m^{-2}. Two different electrodes with 0.08% expander

C_0 (M)	*Discharge capacity (Ah m^{-2})*
1	65, 71
3	175, 187
5	225, 232

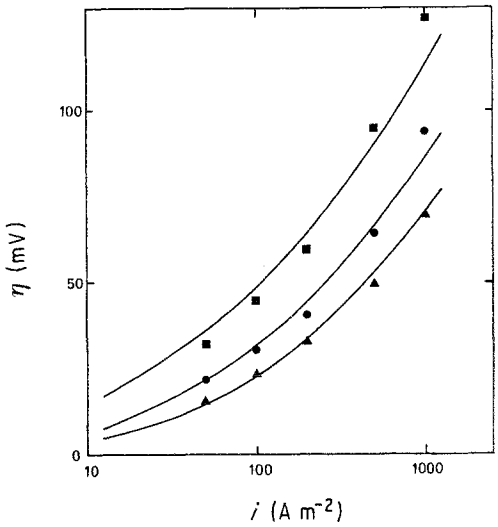

Fig. 2. Polarization curves for electrode with 0.3% expander at different states of discharge. Experimental points: ▲ $q = 60\,\mathrm{Ah\,m^{-2}}$; ● $q = 210\,\mathrm{Ah\,m^{-2}}$; ■ $q = 320\,\mathrm{Ah\,m^{-2}}$; $q_d = 380\,\mathrm{Ah\,m^{-2}}$. The lines are calculated from Equations 4–6 with $(j^c_{lim})^0 = -5 \times 10^4\,\mathrm{A\,m^{-3}}$, $(S_2 J_0)^0 = 1.4 \times 10^5\,\mathrm{A\,m^{-3}}$ and $m = 1$.

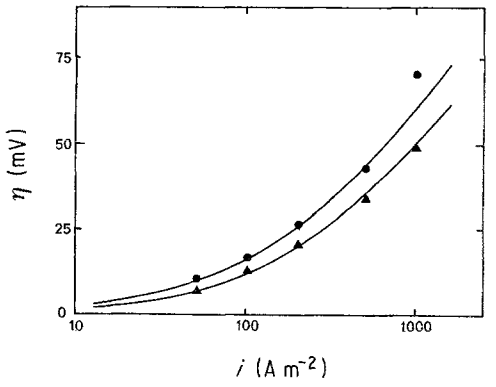

Fig. 4. Polarization curves for electrode without expander at different states of discharge. Experimental points: ▲ $q = 60\,\mathrm{Ah\,m^{-2}}$; ● $q = 210\,\mathrm{Ah\,m^{-2}}$; $q_d = 293\,\mathrm{Ah\,m^{-2}}$. The lines are calculated from Equations 4–6 with $(j^c_{lim})^0 = -1.2 \times 10^5\,\mathrm{A\,m^{-3}}$, $(S_2 J_0)^0 = 6 \times 10^5\,\mathrm{A\,m^{-3}}$ and $m = 0.5$.

trodes at different states of discharge are shown in Figs 2–4. In between these measurements the electrodes were discharged with a low current density ($20\,\mathrm{A\,m^{-2}}$) to obtain a uniform current distribution and to avoid concentration gradients. For the electrode without expander it was not possible to obtain polarization curves when discharged to more than 50% at $20\,\mathrm{A\,m^{-2}}$, since when a high current density was applied at this state of discharge the electrode potential rapidly broke down.

Figure 5 shows the anodic polarization curve for a fully charged electrode on which the current was applied on one side only. The overvoltage was measured both at the front and the back of the electrode. The electrode was given an excessive charge between the current steps. In this way it was possible to hold the active surface area of lead constant and free from lead sulphate for all points of the polarization curves.

The measured polarization curves for the porous lead electrode are determined both by the local activity as a function of the structure and the current distribution along the depth of the electrode. A kinetic expression for the recharge process of the lead electrode has been derived previously [37]. The expression is based on a mechanism involving dissolution of lead sulphate, diffusion of lead ions and electrodeposition. This expression can also be tested for the discharge process. The relation between the current density j in $\mathrm{A\,m^{-3}}$ and the overvoltage η can then be written [37]

$$j = \frac{j^c_{lim}\,(1 - \exp(2\eta'))}{1 - j^c_{lim} \exp(\alpha_c \eta')/(S_2 J_0)} \qquad (1)$$

where $\eta' = F\eta/RT$, S_2 is the specific active surface area of lead, J_0 is the true exchange current density and j^c_{lim} is the limiting current density for the cathodic reaction according to the relation [37]

$$-\frac{1}{j^c_{lim}} = \frac{1}{2Fk_0 S_1} + \frac{1}{2Fk_m S_m c_{eq}} \qquad (2)$$

where k_0 is a dissolution rate constant, S_1 is the specific active surface area of lead sulphate, k_m is an averaged

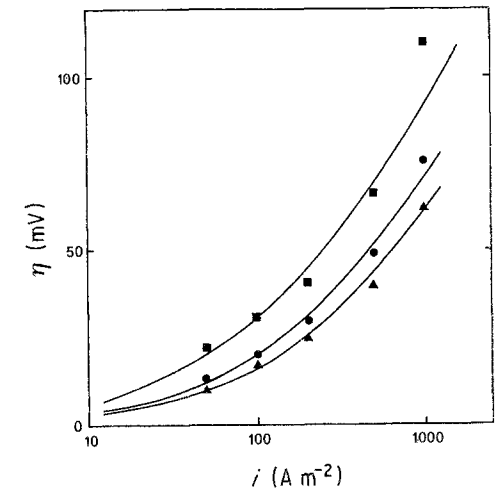

Fig. 3. Polarization curves for electrode with 0.08% expander at different states of discharge. Experimental points: ▲ $q = 60\,\mathrm{Ah\,m^{-2}}$; ● $q = 210\,\mathrm{Ah\,m^{-2}}$; ■ $q = 330\,\mathrm{Ah\,m^{-2}}$; $q_d = 370\,\mathrm{Ah\,m^{-2}}$. The lines are calculated from Equations 4–6 with $(j^c_{lim})^0 = -10^5\,\mathrm{A\,m^{-3}}$, $(S_2 J_0)^0 = 1.9 \times 10^5\,\mathrm{A\,m^{-3}}$ and $m = 0.5$.

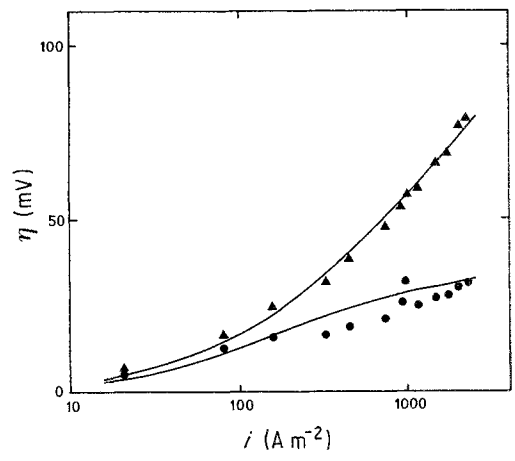

Fig. 5. Polarization curve for fully charged electrode with 0.08% expander. Current from only one side. Experimental points: ▲ front side; ● back side. The curves are calculated with Equations 3–5 with $(j^c_{lim})^0 = -2.5 \times 10^4\,\mathrm{A\,m^{-3}}$, $(S_2 J_0)^0 = 5 \times 10^6\,\mathrm{A\,m^{-3}}$, $\kappa = 23\,\Omega^{-1}\,\mathrm{m^{-1}}$, $L = 0.002\,\mathrm{m}$.

mass transfer coefficient, S_m is a mean effective cross section area for the diffusion of lead ions and c_{eq} is the saturation concentration of lead ions.

In Equation 2 the cathodic limiting current density is determined by the dissolution rate of lead sulphate and diffusion of lead ions from lead sulphate crystals to lead growth sites, respectively. In the anodic case $-j^c_{lim}$ is instead a measure of the influence of diffusion of lead ions from an electroactive lead surface to a growth site on a lead sulphate crystal and/or the kinetics of precipitation of lead sulphate. If $-j^c_{lim} \gg S_2 J_0$ the diffusion rate and crystallization kinetics are fast compared to the electrode kinetics, and Equation 1 is transformed into the ordinary Butler–Volmer equation with an anodic transfer coefficient of $(2 - \alpha_c)$. When $-j^c_{lim} \ll S_2 J_0$ Equation 1 tends to the expression

$$j = -j^c_{lim} (\exp (2\eta') - 1) \quad (3)$$

for small values of η', and again to the ordinary Butler–Volmer equation at higher overvoltages. This means that the diffusion of lead ions and/or the precipitation of lead sulphate through solution is the rate-determining step at lower overvoltages, which corresponds to a Tafel slope of 30 mV according to Equation 3, while the charge transfer reaction is the rate determining step at higher overvoltages.

Figures 2–4 show that the polarization curves are shifted with the extent of discharge in a way which indicates that due to the structural changes both $S_2 J_0$ and $-j^c_{lim}$ decrease during discharge and in approximately the same way. An explicit dependence on the extent of discharge can then be introduced in Equation 1 in the following way

$$j = \frac{(S_2 J_0)^0 (1 - \exp (2\eta')) (1 - q/q_d)^m}{(S_2 J_0 / j^c_{lim})^0 - \exp (\alpha_c \eta')} \quad (4)$$

where q is the actual charge output in (Ah m^{-2}) and q_d is the same quantity after a completed discharge. Index 0 denotes initial values. The changes in structural dependences of the kinetic parameters in the denominator vanish because of the assumption that they are approximately the same for the parameters S_2 and j^c_{lim}. The exponent m is a fitting parameter which from Figs 2 and 3 could be estimated to be about 1 for the electrode with 0.3% expander and about 0.5 for the electrodes with 0.08% or without expander. The polarization curves can be calculated from Equation 4 coupled with an equation for the ionic current density in the electrolyte phase

$$i_e = \kappa \partial \eta / \partial x \quad (5)$$

and an equation for the change in this current density due to the charge transfer reaction

$$\partial i_e / \partial x = j \quad (6)$$

Equation 5 is valid under the assumptions that the conductivity of the solid phase is much higher than that of the electrolyte and that the concentration gradient of sulphuric acid can be neglected. The value of the effective conductivity, κ, was taken to be $20\,\Omega^{-1}\,m^{-1}$ for the electrode discharged to about 20%, $15\,\Omega^{-1}\,m^{-1}$ for the electrode discharged to about 50% and $10\,\Omega\,m^{-1}$ for the electrode discharged to about 80% according to the results presented below.

The boundary conditions are $i_e = 0$ at the symmetry plane of the electrode, $x = 0$ and $i_e = i$ at the exterior surface, $x = L$, where i is the apparent geometric current density. Equations 4–6 were solved numerically with j^c_{lim} and $S_2 J_0$ as fitting parameters. The value of α_c was taken to be 0.9 as obtained from the cathodic polarization curves [37].

The predicted polarization curves are drawn as solid lines in Figs 2–5. These fits have been obtained with values of the parameter $S_2 J_0$ which for Figs 2 and 3 are within the same region as found for the recharge process of the lead electrodes without expander [37] and with 0.08% expander [38] but an order of magnitude larger than for the electrode with 0.3% expander [37]. The value of j^c_{lim} is approximately the same as in the beginning of the recharge process [3] for the electrode with 0.3% expander (Fig. 2). For the factory-manufacted electrode with 0.08% expander, Fig. 3, the value of j^c_{lim} is in the same region as for this electrode and the electrode without expander at the end of the recharge process. For the electrode without expander $S_2 J_0$ is 3–4 times higher than for the electrodes with expander, while j^c_{lim} is only slightly higher than for the electrode with 0.08% expander.

The fitted curves show good agreement with the experimental points except at the highest current density at the highest extent of discharge. This deviation may be ascribed, at least partly, to a rapid change of the surface conditions during the polarization measurements. The points were taken in the order from lower to higher current densities. For the highest current density at the highest extent of discharge, the electrode potential increased rapidly during the time (0.5 min) of measurement, probably due to an accelerated passivation of the electroactive surface by lead sulphate.

3.3. *Structural changes*

During the discharge process Pb transforms to $PbSO_4$ which has a 2.7 times larger molar volume. This leads to a plugging of the pores in the porous electrode and the obstruction of the transport of ions in the pores. To determine the effect of pore plugging, the effective conductivity in the pores was measured at different states of discharge. The electrode was discharged with a low current density to obtain a uniform distribution of $PbSO_4$ and to avoid concentration gradients. The measurements were performed by applying a constant current density between two counter electrodes and recording the potential drop across the working electrode with one reference electrode on each side of the electrode. This method has the disadvantage that a fraction of the current may pass through the solid electrode phase by a bipolar mechanism [39]. The fraction of current that passes through the solid electrode phase was calculated to be less than 10%. For the fully charged electrodes, which contain no lead

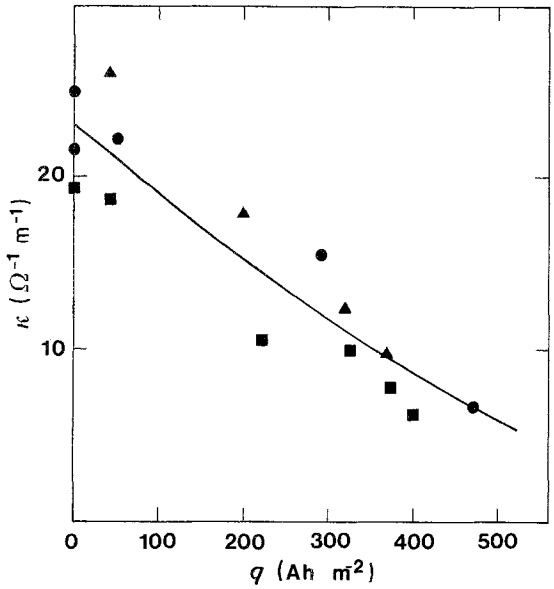

Fig. 6. Changes in effective conductivity during discharge for the different electrodes: ▲ electrode with 0.3% expander; ● electrode with 0.08% expander; ■ electrode without expander.

sulphate as reactant for the cathodic reaction, and for the fully discharged electrodes, in which the anodic reaction is hindered, this fraction should be considerably smaller. Figure 6 shows how the effective conductivity changes between the different electrodes and also between different cycles for the same electrode. In Fig. 6 a curve is drawn corresponding to the Bruggeman relation

$$\frac{\kappa}{\kappa_0} = \left(\frac{\varepsilon}{\varepsilon_0}\right)^{1.5} \tag{7}$$

where ε = porosity of the electrode
ε_0 = initial porosity
κ_0 = initial effective conductivity.

The initial porosity was determined from titrations on the pore electrolyte as 0.6.

The size of the lead sulphate crystals in the electrodes with expander is about 1 to a few μm, see Figs 7 and 8. In the electrode with 0.3% expander they are more regularly shaped than in the electrode with 0.08% expander, where the crystals are more irregular. In the electrodes without expander the crystals are

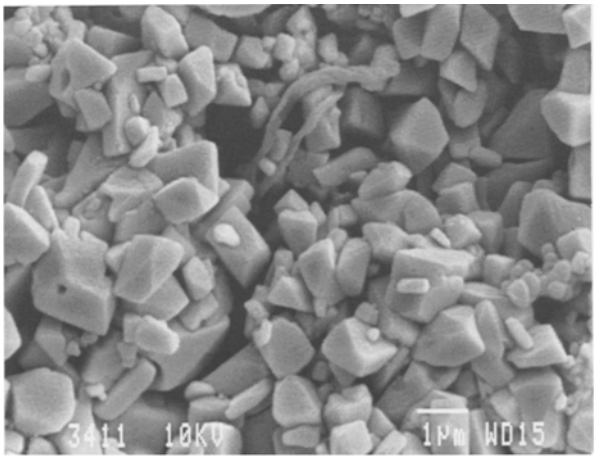

Fig. 7. Morphology of the interior of an electrode with 0.3% expander. Discharged with 1000 A m^{-2}.

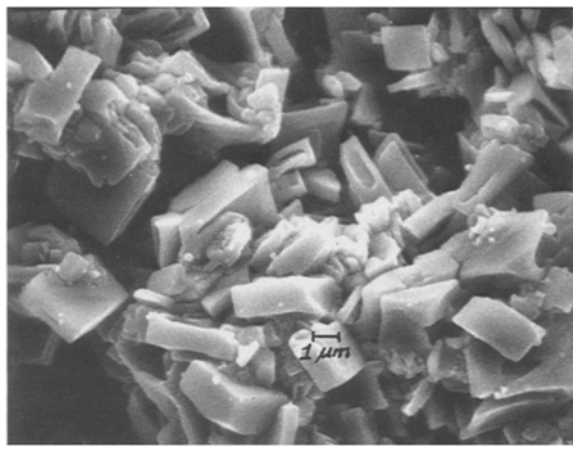

Fig. 8. Morphology of the interior of an electrode with 0.08% expander. Discharged with 1000 A m^{-2}.

generally much smaller and in some parts the surface seems to be covered rather with a lead sulphate film, see Fig. 9 and also Fig. 9 in [38]. On the exterior surface of the electrodes with 0.08% expander two different types of structures could be observed at different parts of the electrode. At one the external surface was completely covered with lead sulphate crystals of a size of about one μm (see Fig. 10). The other type of structure consists of much smaller crystals gathered on the surface of what may be larger lead particles (see Fig. 11).

The lead sulphate distribution across the electrodes discharged with a low current density is uniform both for electrodes with 0.3% and without expander [37]. The results of the electron probe microanalyses of electrodes discharged with 1000 A m^{-2} are shown in Fig. 12. In the electrode without expander the lead sulphate concentration is low and its distribution is uniform. The electrode with 0.3% expander shows a maximum of lead sulphate in the centre of the electrode. For the electrode with 0.08% expander the lead sulphate distribution is different for different cross sections of the electrode as shown in Fig. 13. At some points the amount of lead sulphate is highest in the centre of the electrode, whereas at other points there is a minimum of lead sulphate in the centre of the electrode.

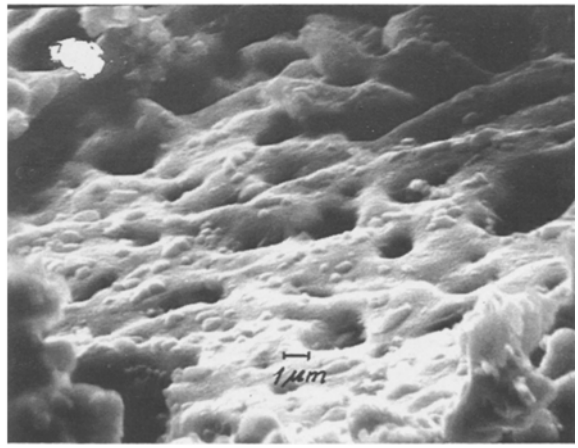

Fig. 9. Morphology of the interior of an electrode without expander. Discharged with 1000 A m^{-2}.

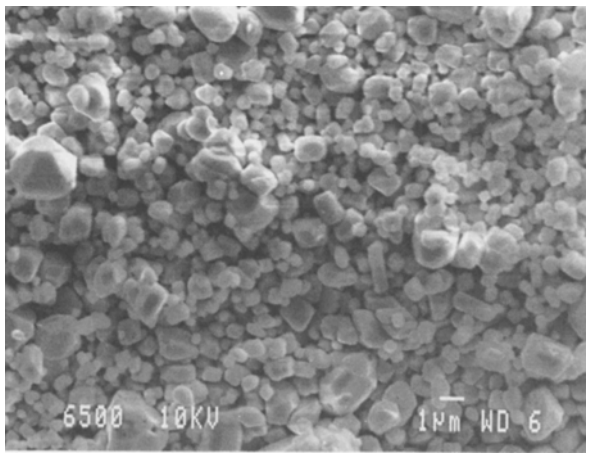

Fig. 10. SEM micrograph showing an area with closely packed lead sulphate crystals on the exterior surface of an electrode with 0.08% expander.

4. Discussion

The experimental results show that the effect of the expander on the discharge capacity is largest at high rates of discharge. The low discharge capacity of the electrode without expander at the highest current density (Fig. 1) can be explained by a rapid covering of the lead surface with very small crystals or a film of lead sulphate as shown by Fig. 9. This leads to a low mass utilization, which in turn leads to a uniform lead sulphate distribution across the electrode at the end of the complete discharge, Fig. 12, since neither blocking of the pores nor sulphuric acid depletion will hinder the full utilization of the interior parts. In contrast, the lead sulphate distribution across the electrode with a high concentration of expander shows a maximum in the centre of the electrode (Fig. 12), which indicates that its capacity is also limited by the coverage of the active surface area of lead by lead sulphate. The high concentration of lead sulphate in the centre of the electrode can be explained by the fact that the sulphuric acid concentration is lower in the centre of the electrode during discharge, which leads to larger lead sulphate crystals and thus a larger amount of lead sulphate before the active lead surface is covered [19].

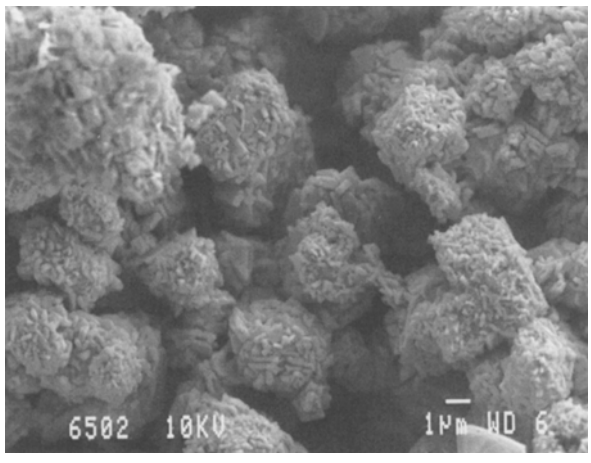

Fig. 11. SEM micrograph showing an area with agglomerates of small lead sulphate crystals on the exterior surface of an electrode with 0.08% expander.

It is interesting to note from Figs 12 and 13 that in no case does the lead sulphate distribution have its maximum at the exterior surface, as would be expected with consideration of elementary rules for the current density distribution. The maximum instead appears at some distance into the interior of the electrode. This observation can be compared with similar lead sulphate distribution curves for electrodes which have been fully discharged with a low current density [37] or a medium current density [7], which do not exhibit this type of maximum. A possible explanation is that the maximum possible local mass utilization is a function not only of sulphuric acid concentration, but also of the local current density. It is well known that a higher current density leads to a lower mass utilization even for planar electrodes [37]. Since the initial current distribution will have a pronounced maximum at the exterior surface, the local current density will be very high in the outer parts of the electrode, which will therefore be deactivated more rapidly by smaller lead sulphate crystals. The higher overvoltage in these outer parts of the electrode may also favour the solid state formation of lead sulphate, which would give a more rapid passivation of the electrode surface in these parts than in the interior of the electrode, where the dissolution–precipitation mechanism may still predominate.

An alternative explanation of the anomalous lead sulphate distributions would be that the lead sulphate is redistributed by the washing procedure as previously demonstrated for washing a partially discharged lead dioxide electrode with water [40]. In this work acetone was chosen instead of water on the assumption that the redistribution effect is less important with this solvent. This assumption was checked indirectly by washing a sample from only one side, the other side being covered by a rubber cloth pressed to it. A redistribution effect due to concentration cells would then result in a significantly asymmetric distribution of lead sulphate across the thickness of the plate. Especially, an original peak at the exterior surface would be diminished at the front side and increased at the back side. As shown in Fig. 13 this was not the case, and the redistribution effect can thus be neglected.

The great differences in lead sulphate distribution between different cross sections of the electrode with standard concentration of expander (Fig. 13) indicate that this electrode is inhomogeneous with respect to the structural transformations. It is not possible on the basis of the present information to determine the reason for this inhomogeneity, although a simple explanation would be that the expander is non-uniformly distributed over the electrode. The variation in the lead sulphate distribution indicates that different mechanisms may limit the discharge capacity at different parts of the electrode. At the points where the lead sulphate concentration has a maximum in the centre of the electrode, the discharge capacity is probably limited by the coverage of the active surface area of lead by lead sulphate as in the electrode with 0.3% expander. At the points where the lead sulphate con-

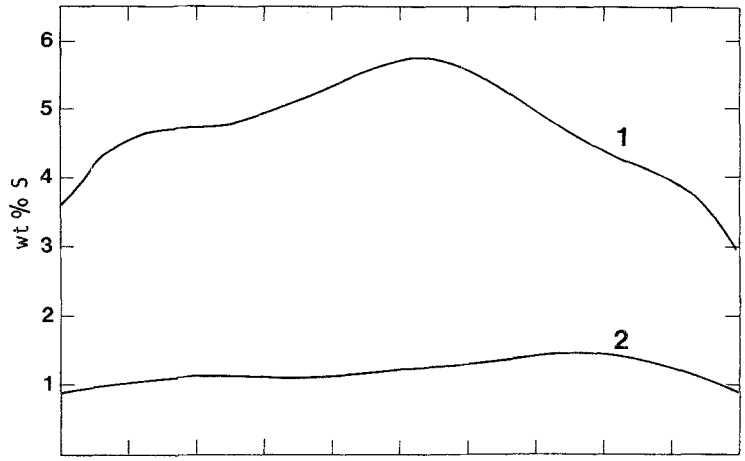

Fig. 12. Sulphur distribution across the thickness of a porous lead electrode discharged with 1000 A m^{-2}. (1) Electrode with 0.3% expander; (2) electrode without expander.

centration instead shows a minimum in the centre of the electrode, the capacity is limited by either a local depletion of sulphuric acid in the pores or a pore blocking effect. Sulphuric acid can only have been depleted locally since the average concentration of sulphuric acid in the pores after a discharge with 1000 A m^{-2} was measured to 3.0 M. Asai *et al.* [7] have reported similar curves for the $PbSO_4$ distribution, which show an incomplete utilization of the interior of the electrode even at the comparatively low current density of 200 A m^{-2}. They also measured a rapid increase of the ionic resistance through the electrode at the end of discharge and concluded that the discharge has been limited by plugging of the pore entrances. The SEM studies showed that some parts of the exterior surface are completely covered with densely packed lead sulphate crystals, see Fig. 10. This structure may be dense enough to block the underlying pores, while the coarser pores in Fig. 11 cannot be plugged by the smaller lead sulphate crystals. This latter structure may be explained by a local concentration of organic expander which is too low.

From the values of the parameters which give good fits using Equation 3 to experimental polarization curves in Figs 2–4 it is evident that especially the electrode kinetics but also the transport of lead ions are impeded by the expander. The effect of an increase in the expander concentration from 0 to 0.3% on the intrinsic electrode kinetics is a 4-fold reduction of the value of the parameter $S_2 J_0$ which is to be compared with a 10–20-fold reduction of $S_2 J_0$ for the recharge process [37].

Since S_2, the active surface area of lead, is more than twice as high in the electrode with 0.3% expander as in the electrode without expander [37], the true exchange current density J_0 is about 8 times lower in the electrode with 0.3% expander. This reduction can be explained by a blockage of the surface of lead by the absorbed expander. The value of the parameter j^c_{lim}, which in the anodic case is a measure of the diffusion rate of lead ions and/or the crystallization rate of $PbSO_4$, is reduced 3–5 times when the expander concentration is increased from 0 to 0.3%. For the cathodic reaction the parameter j^c_{lim} is the limiting current density due to a limiting diffusion rate of lead ions [38]. In the cathodic case the reduction of the value of the parameter j^c_{lim} is also by a factor of 3–5 when the expander concentration increases from 0 to 0.3% [37].

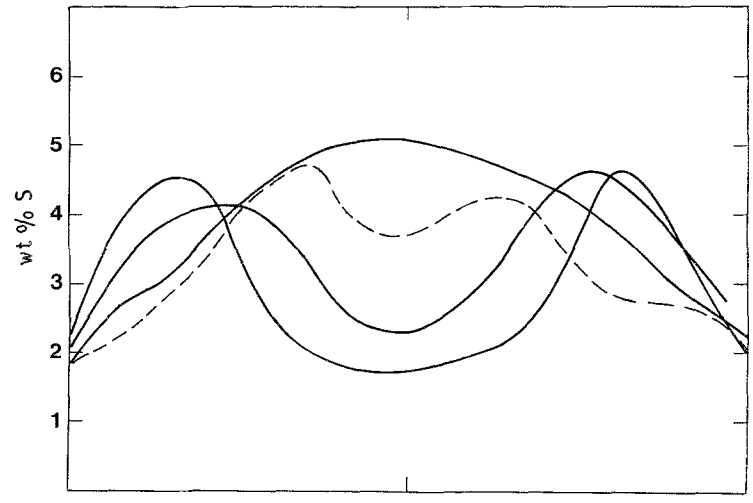

Fig. 13. Sulphur distribution across the thickness of a porous electrode with 0.08% expander. Discharge current 1000 A m^{-2}. The different curves are from the same electrode but different points. Dashed line: sample washed from the right hand side only.

The meaning and importance of the parameter j_{lim}^{c} is clearly illustrated by the polarization curve for the fully charged electrode with 0.08% expander in Fig. 5. By applying the current from only one side and measuring the electrode potential on both sides of the electrode, more direct information on the current density distribution and a better test of the kinetic model are obtained. The theoretical prediction by the use of Equations 3–5 is reasonably good for $j_{lim}^{c} = -2.5 \times 10^4\,A\,m^{-3}$ and $S_2 J_0 \geqslant 5 \times 10^6\,A\,m^{-3}$. The first value is only a quarter of that obtained from the fits in Fig. 3 for the same electrode after discharge to different extents. This can be explained by the fact that there are no nuclei of lead sulphate present in the electrode when the current is switched on to measure the overvoltage at a given current density. The kinetics will then be determined by the crystallization process for the precipitation of lead sulphate. This is also reflected in the galvanostatic discharge curves for the electrodes with expander at high rates of discharge, which exhibit an initial voltage dip, see Fig. 1. If the crystallization process is first order with respect to the concentration of lead ions, as is assumed in Equation 2 [37], j_{lim}^{c} is proportional to a rate constant for the crystallization process. Since $-j_{lim}^{c} \ll S_2 J_0$ the electrode kinetics are to be regarded as practically reversible, and Equation 4 is reduced to Equation 3, which in this case describes the anodic process as limited by the rate of crystallization of lead sulphate. According to Equation 3 a Tafel slope of 30 mV should be expected for the intrinsic kinetics. The very high non-uniformity of the current density distribution makes the apparent Tafel slope of the porous electrode almost doubled.

The value of $S_2 J_0$ predicted from Fig. 5 is much higher than those predicted for the same electrode at partial discharges, Fig. 3. This can be explained by the fact that the surface area is completely free from lead sulphate. A comparison with Fig. 3 gives that the value of $S_2 J_0$ decreases by an order of magnitude when the electrode is discharged to only 16%. This can only be explained by the formation of a film of lead sulphate rather than the formation of larger lead sulphate crystals. Both structures can probably be obtained simultaneously, as discussed in [38].

Further support for the assumption of film formation even under conditions with dissolution–precipitation as the predominating mechanism has been given by Stange [41], who concluded from SEM studies that an amorphous film of lead sulphate is formed in a primary stage, while well-known $PbSO_4$ crystals develop in a second stage. The thickening and densification of this film with the extent of discharge can explain the decreasing value of j_{lim}^{c} (Fig. 3) which is now determined mainly by the diffusion rate of lead ions through the presumably porous film. This would also explain why the variation of j_{lim}^{c} with the state of discharge is opposite to that during recharge, where j_{lim}^{c} decreases with the amount of lead sulphate. Since the lead sulphate film is removed in the initial part of the recharge process [38], Equation 1 then describes dissolution of well-shaped lead sulphate crystals, diffusion of lead ions through the pore electrolyte and electrodeposition at a growth site on the lead surface and does not include diffusion of lead ions through a porous film. A decreasing porosity of the film would also explain how the value of S_2 can decrease at approximately the same rate as j_{lim}^{c}, as assumed in Equation 4.

5. Conclusions

The studies reported above have shown that the addition of lignosulphonate expander increases the discharge capacity considerably, especially at high current densities, due to an increased active material utilization, which in turn can be attributed to the formation of larger lead sulphate crystals. At low rates of discharge the organic expander does not increase the discharge capacity significantly, since in this case equally large lead sulphate crystals are formed in the dissolution–precipitation mechanism even without expander.

The polarization curves at different states of discharge can be fitted by a rate expression, which takes into account the anodic dissolution of lead, the diffusion of lead ions and crystallization of lead sulphate, respectively.

The variation of the parameters in the model with the extent of discharge can be explained by the formation of a porous film of lead sulphate even under conditions where the diffusion–precipitation mechanism predominates.

Acknowledgement

This work was financially supported by The National Swedish Board for Technical Development (Project No. 83-3262).

References

[1] N. A. Hampson and J. B. Lakeman, *J. Power Sources* **6** (1981) 101.
[2] B. K. Mahato, *Prog. Batteries Solar Cells* **5** (1984) 212.
[3] D. Pavlov, in 'Power Sources for Electric Vehicles' (edited by McNicol and D. A. J. Rand), Elsevier, Amsterdam (1984).
[4] J. Burbank, A. C. Simon and E. Willihnganz, in 'Adv. Electrochem. and Electrochem. Eng.' (edited by P. Delahay and C. W. Tobias), Vol. 8 (1971) p. 157.
[5] U. Hullmeine and W. Kappus, *Electrochim. Acta* **27** (1982) 1677.
[6] A. Winsel, U. Hullmeine and E. Voss, *J. Power Sources* **2** (1977/1978) 369.
[7] K. Asai, M. Tsubota, K. Yonezu and K. Ando, Preprint from 14th international Power Sources Symposium, Brighton (1984).
[8] B. K. Mahato, *J. Electrochem. Soc.* **124** (1977) 124.
[9] J. R. Pierson, P. Gurlusky, A. C. Simon and S. M. Caulder, *J. Electrochem. Soc.* **117** (1970) 1463.
[10] A. C. Simon, S. M. Caulder, P. J. Gurlusky and P. J. Pierson, *ibid.* **121** (1974) 463.
[11] E. Willihnganz, *Trans. Electrochem. Soc.* **92** (1947) 281.
[12] M. P. J. Brennan and N. A. Hampson, *J. Electroanal. Chem.* **48** (1973) 465.
[13] B. K. Mahato, *J. Electrochem. Soc.* **128** (1981) 1416.
[14] V. Iliev and D. Pavlov, *J. Appl. Electrochem.* **15** (1985) 39.
[15] G. Hoffman and W. Vielstich, *J. Electroanal. Chem.* **180** (1984) 565.

[16] B. K. Mahato, *J. Electrochem. Soc.* **127** (1980) 1679.
[17] E. G. Yampolskaya, M. I. Ershova, I. I. Astakov and B. N. Kabanov, *Elektrokhimiya* **2** (1966) 1327.
[18] E. G. Yampolskaya, M. I. Ershova, V. V. Surikov, I. I. Astakov and B. N. Kabanov, *Elektrokhimiya* **8** (1972) 1236.
[19] K. Asai, M. Tsubota, K. Yonezu and K. Ando, *J. Power Sources* **7** (1981) 73.
[20] G. Archdale and J. A. Harrison, *J. Electroanal. Chem.* **47** (1973) 93.
[21] B. N. Kabanov, in 'Proceedings of Second Conference in Metal Corrosion', Vol. 2 (in Russian) Izd. Akad. Nauk SSSR, Moscow (1943) p. 67.
[22] G. Archdale and J. A. Harrison, *J. Electroanal. Chem.* **34** (1972) 21.
[23] G. Archdale and J. A. Harrison, *J. Electroanal. Chem.* **39** (1972) 357.
[24] G. Archdale and J. A. Harrison, *J. Electroanal. Chem.* **43** (1973) 321.
[25] M. P. J. Brennan and N. A. Hampson, *J. Electroanal. Chem.* **52** (1974) 1.
[26] A. N. Fleming and J. A. Harrison, *Electrochim. Acta* **21** (1976) 905.
[27] S. Fletcher and D. B. Natthews, *J. Appl. Electrochem.* **11** (1981) 23.
[28] N. A. Hampson and J. B. Lakeman, *J. Electroanal. Chem.* **112** (1980) 355.
[29] N. A. Hampson and J. B. Lakeman, *J. Power Sources* **4** (1979) 21.
[30] N. A. Hampson and J. B. Lakeman, *J. Appl. Electrochem.* **9** (1979) 403.
[31] N. A. Hampson and J. B. Lakeman, *J. Electroanal. Chem.* **107** (1980) 177.
[32] N. A. Hampson and J. B. Lakeman, *J. Electroanal. Chem.* **108** (1980) 108.
[33] N. A. Hampson and J. B. Lakeman, *J. Electroanal. Chem.* **119** (1981) 3.
[34] D. Pavlov and V. Iliev, *J. Power Sources* **7** (1981/1982) 153.
[35] M. S. Panesar and V. Portscher, *Metall. Angew. Elektrochem.* **26** (1972) 252.
[36] W. Kappus and A. Winsel, *J. Power Sources* **8** (1982) 159.
[37] P. Ekdunge, K. V. Rybalka and D. Simonsson, *Electrochim. Acta* **32** (1987) 659.
[38] P. Ekdunge, M. Lindgren and D. Simonsson, *J. Electrochem. Soc.* **135** (1988) 1613.
[39] F. A. Posey and S. S. Misra, *J. Electrochem. Soc.* **113** (1966) 608.
[40] D. Simonsson, *J. Electrochem. Soc.* **120** (1973) 151.
[41] J. Stange, *Electrochim. Acta* **19** (1974) 111.